Ultimate Strength Considerations for Seismic Design of the Reduced Beam Section (Internal Plastic Hinge)

NESTOR IWANKIW, AISC

Several international (Ref. 1–4) and more recent US (Ref. 5 & 6) research tests have confirmed that the use of a reduced section (often referred to as "dogbone") of a wide flange beam in the proximity of welded beam-to-column moment connections is a very promising means to improve seismic ductility. The notion to protect against seismic overloads through an intentional ductile "fuse" has long existed, but this particular application has recently surfaced as an alternative solution to the post-Northridge concerns about the prescriptive welded connection detail. ARBED, the owner of a 1992 US patent on the reduced beam section (RBS), has graciously waived any commercial royalty rights for its public use.

The RBS is accomplished through an engineered gradual transition of the beam flanges to the intended reduced section at a given location. In comparison to the reinforced (strengthened) connections with beam cover plates, ribs, side plates, or haunches, this modification provides the more reliable ductility of "interior" plastic hinge formation in the main beam member but without elevating force demands on the supporting columns and the remaining framing system beyond those of the original member sizes. Likewise, this efficient configuration does not increase the required weld deposition volume, constraint, nor supplementary material requirements.

Further analysis and testing of this relatively new concept for controlled beam yielding is proceeding to better define the geometry of the reduced wide flange section detail itself, practical limits on relevant variables, effects of the composite floor slab, lateral bracing, and implications, if any, on the overall strength and serviceability (drift) of the building frame. Due to the lack of explicit detailing criteria, the following discussion is an initial attempt to develop normalized design considerations for the size and placement of the reduced beam section. These were originally developed in conjunction with the sizing of specimens for the research tests in Ref. 5. The underlying strength and equilibrium principles may be extended to other seismic details that have been successfully tested and which shift the plastic hinge to the interior of the beam. Further calibration is expected from the emerging empirical evidence. To date, the available test data generally confirms the basic design assumptions and expected ductile performance of this new RBS detail through a range including heavier beam sections up to about 200 lb/ft.

The information contained herein is not intended to represent official attitudes, recommendations, or policies of the Institute. While it is believed to be accurate, it should not be used for any specific application without competent professional examination and verification by a licensed professional engineer. Anyone making use of this information assumes all liability from such use.

Nestor Iwankiw is Vice President, Engineering & Research Dept., AISC, Chicago, IL.

PROFILE & LOCATION

The 1994 University of Texas-Austin tests of coverplated connections (Ref. 7) sponsored by AISC and subsequent tests of other reinforced details indicated that formation of a beam plastic hinge at about $d/2$ clear end distance (d being the beam depth) away from the connection to the column will improve seismic ductility by:

1. minimizing the effects of material strength variations, stress concentrations, and other complexities at the beam end connection by limiting it to nominally elastic behavior; in accordance with the classical St. Venant's principle, local effects at member ends and load points are dissipated to a relatively uniform state over a distance equal to about the width of the member, (b_f for a wide flange), which is approximately ⅓ to ½ of the member depth.
2. maintaining a reasonably small bending moment differential (gradient) between the interior plastic hinge and the beam end (or equivalently, locating plastic hinge section as close as possible to the highest flexural demand)

Testing to date has confirmed that a similar result can be attained with a properly designed and detailed reduced beam section. Fig. 1 schematic illustrates three rational patterns for concentrating the beam inelasticity at e away from the end. The total length of the RBS zone ranges between $0.75d$ to d.

Option 1, is a symmetrical flange cutout with no size distinctions between either of its sides (Refs. 2–4). Option 2, or a "teardrop" pattern (Ref. 1 and 5), provides for maximum flange removal on the interior (span) side and a cutout gradient that more closely matches the linear beam moment gradient for uniform and unconstrained yielding in this region. Both of these profiles attempt to simulate the "necked-down" region of a simple tensile coupon specimen, and similar to tapered flange plates used in some wind connection applications. Alternatively, the flange reduction could be produced with a curved cutout pattern (Option 3). The latter may be the easiest profile to fabricate in larger quantities and it eliminates abrupt geometric discontinuities, which cause stress concentrations (Ref. 6). Thus, it may be the preferred RBS option.

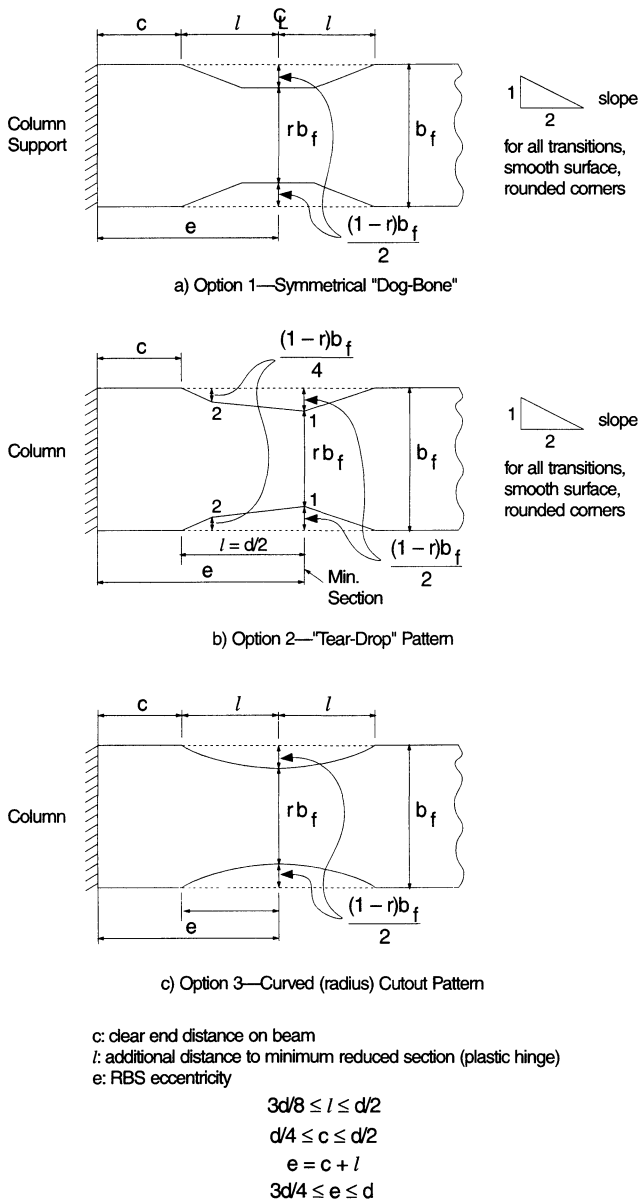

c: clear end distance on beam
l: additional distance to minimum reduced section (plastic hinge)
e: RBS eccentricity

$$3d/8 \le l \le d/2$$
$$d/4 \le c \le d/2$$
$$e = c + l$$
$$3d/4 \le e \le d$$

Fig. 1. Schematic of reduced beam section options.

A smooth contour is imperative for the reduced beam section in any profile. The cut edges should be ground to have a surface roughness value not in excess of 1,000 as defined in ANSI/ASME B46.1. All corners must be rounded. Proper welding procedures, quality control, and filler metal are assumed for the beam-to column connection itself.

Basic continuity of the beam moments (assumed linear diagram for full double curvature under lateral loads) provides the necessary boundary conditions for the design of the internal plastic hinge and the end moment M_c. Figure 2a shows the bending moment variation along half of a beam span ($L/2$), under the usual assumption that the point of inflection occurs at mid-span for such cases. The upper line represents a reinforced end connection, given that the internal hinge develops the full beam M_p, thereby causing an increase in end moment, $M_c > M_p$. The lowest line represents a reduced beam section with flexural strength $m_p < M_p$, which results in an end moment $M_c < M_p$. The intermediate line gives the typical pre-Northridge condition of beam plastic hinging at the end of the member, $M_c = M_p$. This linear bending equilibrium illustrates the fundamental behavior of the reduced beam section in controlling the amount of moment transfer to the beam end. The eccentricity e of the minimum cross section and moment gradient are the two key design variables.

It should be evident from Fig. 2a that increasing e decreases the required m_p (increases the cutout) with everything else constant, and vice versa. Therefore, smaller beam reductions are possible when the interior plastic hinge is closer to the end (smaller e distance).

Steeper moment gradients (smaller L/d), on the other hand, would increase the moment transfer to the column for a constant distance e and a constant m_p.

In summary, the beam end length c is intended to remain nominally elastic for the ductile RBS with the minimum cross-section (assumed plastic hinge location) occurring at an additional distance l toward the span (total distance $e = c + l$ away from beam end.) (see Fig. 1) In reality, some degree of yielding at the beam end has been observed in tests, but at much lower strain levels than in the pre-Northridge detail, since the primary inelastic demand has been shifted to the RBS. The suggested range on e of $0.75d$ to $1.0d$ accomplishes a balance between internalizing unconstrained yielding within the main member itself while still remaining adjacent to the maximum bending moment demand. The test data in Ref. 6 suggest that the lower bound on e could be further decreased to about $0.6d$.

SIZE OF REDUCED SECTION

The bending equilibrium requirement between the interior beam plastic hinge and the supporting column face (Fig. 2b) is as follows:

$$M_c = m_p^{act} + V_p e \quad (1)$$

where

m_p^{act} = actual plastic moment resistance at min. reduced beam section
$= \beta F_y^{act} z$
z = plastic section modulus of beam at min. reduced beam section, in.^{3}
β = material strain hardening factor (assume $1 \le \beta \le 1.1$ for $F_y \ge 50$ ksi)
e = offset of plastic hinge from beam end (assume $3d/4 \le e \le d$), in.
F_y^{act} = actual yield strength of beam, ksi (or expected, $R_y F_y$, where R_y is an average material overstrength factor, $R_y = 1.1$ for $F_y = 50$ ksi)
V_p = beam shear at plastic hinge due to reverse curvature bending that results in m_p^{act} limit state, kips
M_c = moment delivered to supporting column face, kip-in.
$V_p e$ = moment transfer (amplification) due to shear force eccentricity from beam support, kip-in.

The reduced plastic moment m_p^{act} may include a steel strain hardening factor β, which for Grade 50 and stronger shapes is estimated to not exceed 1.1. The actual beam yield strength F_y^{act} is used directly to account for material overstrength. In order to help protect the beam-to-column connection itself, the maximum beam end moment, M_c, delivered to the column is limited to a selected nominal amount per Fig. 2a that is less than the beam flexural strength. A reasonable initial design range for M_c is 90 to 100 percent of first yield:

$$M_c \le C_f M_y^{act} \quad (2)$$

where

M_y^{act} = actual first yield moment resistance at beam end
$= F_y^{act} S$, kip-in.
S = elastic section modulus of steel beam (unreduced), in.^{3}
C_f = yield stress factor at member end; $0.9 \le C_f \le 1.0$

This assumption implies that a maximum nominal stress of $C_f F_y^{act}$ will be transferred to the column at the beam end. Smaller C_f values than 0.9 are expected to require excessive beam section reductions (more than 50 percent). Restricting M_c to at least $0.9 M_y^{act}$ will also result in an acceptable nominal strength level of no less than $0.8 M_p^{nom}$ at the beam end (column face); see later Section "Effects on Overall Design Strength". Additional stress control at the beam end can be imposed by considering a combination detail with light reinforcing attachments. (see Appendix D).

The additional moment transfer (magnification) from the RBS to the beam end due to shear V, can be approximated by the following fixed-end model subjected only to the primary lateral frame loading as in Fig. 2b: (linear reverse curvature bending only with gravity load effects assumed to be secondary)

L = clear beam span between columns
L' = reduced span between interior plastic hinges

from statics:

$$V_p = \frac{2m_p^{act}}{L'} \quad (3)$$

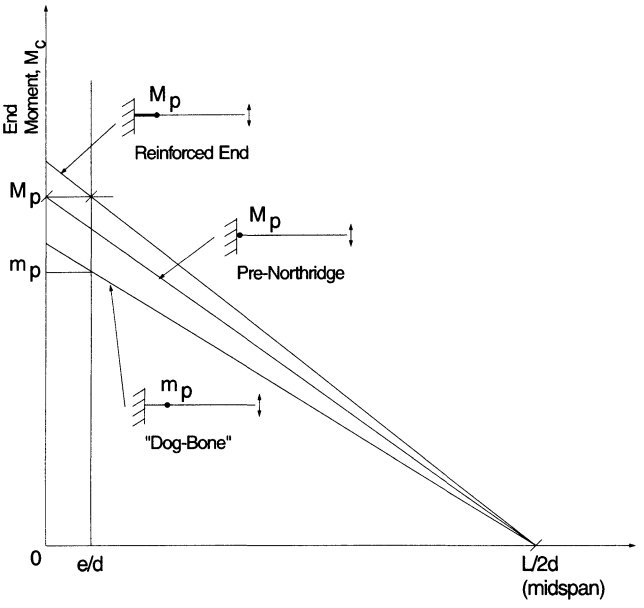

a) Moment Gradient Effect

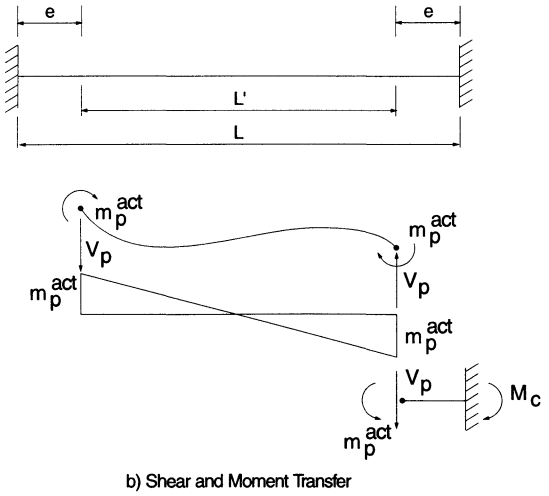

b) Shear and Moment Transfer

Fig. 2. Bending equilibrium (seismic only).

Appendix A contains a more complete discussion of gravity load considerations. The shear coefficient 2 in Equation (3) without gravity will be relabeled, c_v. With gravity effects, c_v will be larger than 2 as discussed in Appendix A.

The RBS design depends on beam L/d (span to depth) ratio and its offset e. For a general solution, using the actual beam L/d ratio, M_c can be computed from Equations (1) and (3) as:

$$L' = L - 2e \tag{4}$$

$$V_p e = \frac{c_v m_p^{act} e}{(L-2e)} = \frac{c_v m_p^{act}\left(\frac{e}{d}\right)}{\left(\frac{L}{d} - 2\left(\frac{e}{d}\right)\right)}$$

(e/d) = normalized eccentricity of interior plastic hinge (assume $\frac{3}{4} \le e/d \le 1$)

c_v = shear force coefficient ≥ 2.0 (App. A)

$$M_c = m_p^{act} + \frac{c_v m_p^{act}\left(\frac{e}{d}\right)}{\left(\frac{L}{d} - 2\left(\frac{e}{d}\right)\right)} \tag{5a}$$

or

$$M_c = m_p^{act}\left[1 + \frac{c_v\left(\frac{e}{d}\right)}{\left(\frac{L}{d} - 2\left(\frac{e}{d}\right)\right)}\right]$$

The second term of the factor is the shear/moment transfer effect which is important for internal plastic hinge designs ($e/d > 0$). The minimum reduced section necessary to maintain nominally elastic ($C_f F_y^{act}$) response at the beam end is provided by:

$$M_c = C_f M_y^{act}$$

or

$$\beta F_y^{act} z\left[1 + \frac{c_v\left(\frac{e}{d}\right)}{\left(\frac{L}{d} - 2\left(\frac{e}{d}\right)\right)}\right] = C_f F_f^{act} S \tag{5b}$$

Dividing by Z and re-arranging results in the following equation that is independent of F_y^{act}:

$$\frac{z}{Z} \le \frac{C_f}{\beta\left[1 + \frac{c_v\left(\frac{e}{d}\right)}{\left(\frac{L}{d} - 2\left(\frac{e}{d}\right)\right)}\right]\left(\frac{Z}{S}\right)}, \quad \frac{L}{d} > 2\left(\frac{e}{d}\right) \tag{6}$$

or

$$\frac{z}{Z} \le \frac{C_f}{\alpha\beta\left(\frac{Z}{S}\right)}$$

where

Z = plastic section modulus of beam

α = moment transfer factor between interior plastic hinge and beam end

$$= \left[1 + \frac{c_v\left(\frac{e}{d}\right)}{\left(\frac{L}{d} - 2\left(\frac{e}{d}\right)\right)}\right] \ge 1.0$$

Even though the beam yield strength has been eliminated in this RBS proportioning, recall that the nominal stress being transmitted to the column will be $C_f F_y^{act}$.

For lateral loads, the shear/moment transfer factor, α, can also be simplified to the ratio (L/L') from use of similar triangles of the linear moment diagram ($c_v = 2.0$). However, this latter span ratio form does not immediately obviate the L/d and e/d design variables as given in the longer alternative expression, and will not be generally accurate with gravity load effects. In Equations (5) & (6), α is the conversion factor relating beam end moment to that of the interior plastic hinge. Because this is a general relationship, (not RBS specific) it is applicable to other interior hinge designs (e.g. cover-plate reinforced, see Appendix B) as well as combination details, see Appendix D.

A serviceability check for $L/d = 20$ is discussed in the 1989 AISC-ASD Commentary, Sect. L3.2, as one means to minimize perceptible floor vibrations. Frame drift limits for regions of high seismicity require increased stiffness and tend to reduce this L/d by about 50 percent to the range of 10. Note that the stiffer, low L/d, beams result in a steeper moment gradient, and therefore, increased section reduction sizes. Larger (e/d) values are also undesirable for the same reason. Since the modified section is accomplished only through beam flange reduction, the required reduced plastic section modulus "z" for the remaining cross-section must be related to this change in the flanges only. Equal (symmetrical) reductions in both flanges of the I-shape are assumed.

For the full original wide flange shape,

$$Z_f + Z_w = Z \tag{7}$$

where

Z_f = plastic section modulus of the beam flanges = $b_f t_f (d - t_f)$, in.^{3}

Z_w = plastic section modulus of the beam web = $(Z - Z_f)$, in.^{3}

b_f, t_f = beam flange width and thickness, respectively, in.

Similarly, for the reduced section:

$$z_f + Z_w = z \tag{8}$$

where

z_f = plastic section modulus of the reduced beam flanges, in.^{3}

or, after nondimensionalizing by division by Z,

$$\frac{z_f}{Z} + \frac{Z_w}{Z} = \frac{z}{Z}$$

where

(z/Z) is the required RBS plastic section modulus defined previously in Equation 6 and
(Z_w/Z) is an I-shape geometric property.

z_f can also be conveniently expressed as:

$$z_f = rb_f t_f (d - t_f) = rZ_f$$

where

r = reduced beam flange width coefficient ≤ 1.0
rb_f = reduced beam flange width (see Fig. 1)

consequently

$$r\left(\frac{Z_f}{Z}\right) + \left(\frac{Z_w}{Z}\right) = \left(\frac{z}{Z}\right) \tag{9}$$

or

$$r = \frac{\left(\frac{z}{Z}\right) - \left(\frac{Z_w}{Z}\right)}{\left(\frac{Z_f}{Z}\right)}$$

gives the purely geometrical relationship for the reduced flange width coefficient "r" based on (z/Z) from Equation (6). The flange width reduction factor is simply $(1 - r)$, which equals

$$(1 - r) = 1 - \left[\frac{\left(\frac{z}{Z}\right) - \left(\frac{Z_w}{Z}\right)}{\left(\frac{Z_f}{Z}\right)}\right] = \frac{1 - \left(\frac{z}{Z}\right)}{\left(\frac{Z_f}{Z}\right)} \tag{10}$$

Equation (9) or Equation (10) can be easily tabulated for several reasonable r, Z_f/Z, and Z_w/Z values for the usual wide-flange proportions to provide an overall illustration of section property changes:

	$(1 - r)$	r	$\left(\frac{Z_f}{Z}\right)$	$\left(\frac{Z_w}{Z}\right)$	$\left(\frac{z}{Z}\right)$
A	(10 percent flange reduction)	0.9	0.8	0.2	0.92
		0.9	0.7	0.3	0.93
		0.9	0.6	0.4	0.94
B	(20 percent flange reduction)	0.8	0.8	0.2	0.84
		0.8	0.7	0.3	0.86
		0.8	0.6	0.4	0.88
C	(30 percent flange reduction)	0.7	0.8	0.2	0.76
		0.7	0.7	0.3	0.79
		0.7	0.6	0.4	0.82
D	(40 percent flange reduction)	0.6	0.8	0.2	0.68
		0.6	0.7	0.3	0.72
		0.6	0.6	0.4	0.76
E	(50 percent flange reduction)	0.5	0.8	0.2	0.60
		0.5	0.7	0.3	0.65
		0.5	0.6	0.4	0.70

Comparing this table with the min (z/Z) based on Equation (6) can quickly provide estimates of the amount of necessary

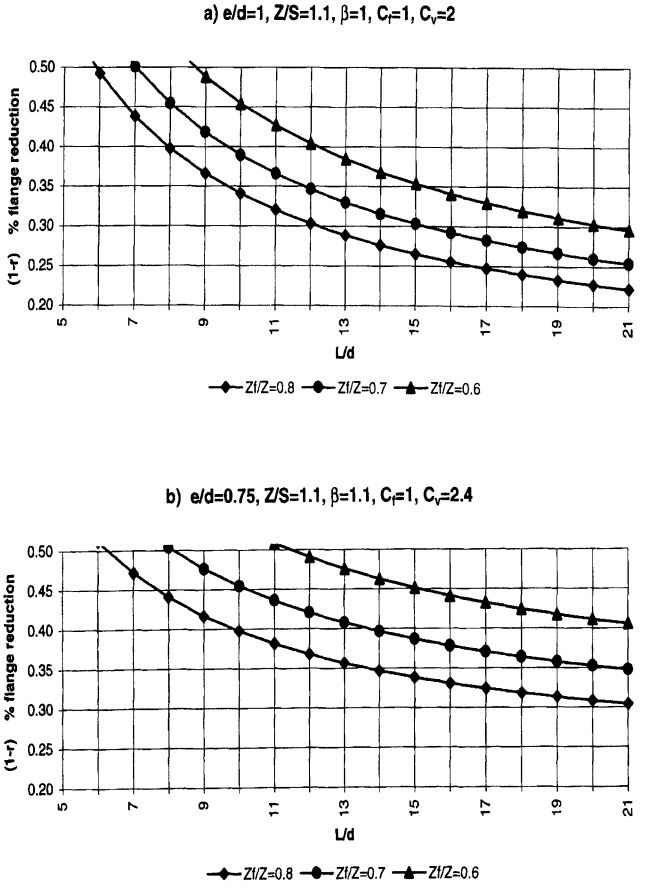

Fig. 3. Reduced beam section variation.

flange reduction. For example, for $L/d = 10$, $e/d = 1$, $\beta = 1$, $C_f = 1$, $Z/S = 1.1$, $c_v = 2$ (no gravity load), and a required $(z/Z) \leq 0.73$, approximately a 40 percent flange reduction is required. Because the flanges are only a part of the beam cross section, the percent flange reduction exceeds its overall (z/Z) shape effect.

Notice that for the results of Equation 9 to be meaningful (positive r), (z/Z) must exceed (Z_w/Z), i.e. the residual plastic modulus "z" cannot be less than Z_w since it is assumed that only the flanges are trimmed. After simplification, this provides another mathematical lower bound limit on L/d with $c_v = 2$:

$$\left(\frac{L}{d}\right)\min = \frac{2\left(\frac{e}{d}\right)C_f}{C_f - \beta\left(\frac{Z_w}{Z}\right)\left(\frac{Z}{S}\right)} \qquad (11)$$

Equation (11) results in minimum (L/d) of about 2–4, thereby mathematically confirming that this lower L/d extreme is to be avoided to maintain the more usual conditions of beam flexure.

The ratios (Z_w/Z) and (Z/S) were left in this common form to enable either general tabulations or charts based on a range of expected values, as well as specific calculations for individual shapes. A plot of the flange reduction $(1-r)$ versus L/d for selected Z_f/Z, e/d values of 1.0 and 0.75, $\beta = 1$ and 1.1, $C_f = 1$, $Z/S = 1.1$, $c_v = 2.0$ and 2.4, is shown in Fig. 3 for general illustration and possible preliminary design. *As cautious interim limits, the reduced beam section should be used only for $L/d > 5$ and $(1-r) < 0.50$ with standard wide-flange sections.*

BEAM END CONNECTION

The development of inelastic strains under cyclic loads in the RBS, and other seismic details that rely on formation of an internal plastic hinge, requires suppression of premature crack initiation at the welded beam end connection, though this shift of primary plasticity demand provides, by itself, some relief to the stress and strain intensity at the flange end connection. All successful full scale RBS testing to date has employed notch tough filler metal (20 ft lbs. at 0° F per CVN) at the beam to column groove welds with removal of the backing bar at the beam bottom flange. Column stiffeners (continuity plates) were also used. Good welding practice and compliance with AWS D1.1, quality control and inspection continue to be important factors in the RBS detail, as in other seismic connections.

The RBS detail presupposes that the beam end connection will transfer 0.9–1.0 of the member's bending moment at first yield ($F_y^{act}S$). RBS tests have been observed to be ductile in sustaining large inelastic rotations with both a fully welded web or a combination bolted/fillet welded shear plate, though some local yielding at the end was evidenced in both cases. No performance differences attributable solely to the beam web connection have been identified to date. The fully welded condition results in a more complete flexural participation of the beam web in force transfer but, likewise, introduces higher joint restraint to residual shrinkage stresses.

DETAILING APPLICATIONS SUMMARY

The following rational procedure has been developed to provide interim guidance in detailing the reduced beam section: (assuming symmetric RBS at both flanges and within beam span (one near each beam end))

1. Select beam reduction profile Option 1, 2 or 3 and C_f, estimate β, establish c and l value, thereby determining (e/d), $\frac{3}{4} \leq e/d \leq 1$; suggest smaller e/d for shorter spans (lower L/d) to minimize moment gradient penalty.
2. For given W-shape and span, L, and L/d, compute α, c_v, Z_f/Z, Z_w/Z, Z/S (see Appendix A for gravity load effects and $c_v > 2$)
3. Solve Equation (6) for (z/Z)
4. Determine flange reduction by Equation 10

$$(1-r) = \frac{\left(1 - \frac{z}{Z}\right)}{\left(\frac{Z_f}{Z}\right)}$$

(steps 3 & 4 can be, of course, combined by simple substitution)

Both for practical and theoretical purposes, interim use of this concept is cautiously limited to $L/d > 5$ (and $e/L \leq 0.20$) and $(1-r) < 0.50$ for standard wide flanges pending further research studies. For many typical design conditions expected in drift-controlled special moment frames, beam flange reduction ratios of 35–45 percent would be expected. Two examples follow.

Example 1

a) Determine reduced section for W30×99 beam, A572-Grade 50, $L/d = 9$, $e/d = 0.75$, $\beta = 1$, $C_f = 1$, $c_v = 2.0$

$d = 29.65$ in. $\quad Z = 312$ in.^{3}
$b_f = 10.45$ in. $\quad S = 269$ in.^{3}
$t_f = 0.67$ in.

$Z_f = (10.45)(0.67)(29.65 - 0.67) = 202.9$ in.^{3}

$$\left(\frac{Z_f}{Z}\right) = \frac{202.9}{312} = 0.65$$

$$\left(\frac{Z}{S}\right) = 1.16$$

$$\left(\frac{Z_w}{Z}\right) = 1 - 0.65 = 0.35$$

Equation (6): $\left(\frac{z}{Z}\right) = \frac{1}{\left[1 + \frac{2(0.75)}{(9 - 2(0.75))}\right](1.16)} = 0.718$

Equation (10): $(1 - r) = \frac{(1 - 0.718)}{0.65} = 0.433$

(about 43 percent flange reduction, or about 4½ – 4¾ in.)

b) repeat a) for L/d = 10 and e/d = 1; (z/Z) = 0.69 & $(1 - r)$ = 0.473 (47 percent flange reduction, or about = 5 in.)

Example 2

a) Determine reduced section for W36×150 beam, A572-Grade 50, L/d = 8, e/d = 0.75, β = 1, C_f = 1, c_v = 2.0

d = 35.85 in. Z = 581 in.^{3}
b_f = 11.98 in. S = 504 in.^{3}
t_f = 0.94 in.

$Z_f = (11.98)(0.94)(35.85 - 0.94) = 393$ in.^{3}

$\left(\frac{Z_f}{Z}\right) = \frac{393}{581} = 0.676$

$\left(\frac{Z}{S}\right) = 1.15$

$\left(\frac{Z_w}{Z}\right) = 1 - 0.676 = 0.324$

Equation (6): $\left(\frac{z}{Z}\right) = \frac{1}{\left[1 + \frac{2(0.75)}{(8 - 2(0.75))}\right](1.15)} = 0.707$

Equation (10): $(1 - r) = \frac{1 - 0.707}{0.676} = 0.433$

(43 percent flange reduction required, about 5¼ in.)

b) repeat a) for L/d = 10 and (e/d) = 1; (z/Z) = 0.696 & $(1 - r)$ = 0.45 (45 percent flange reduction, about 5½ in.)

EFFECTS ON OVERALL DESIGN STRENGTH

Even though drift, not strength, often governs the design of steel moment frames in high seismic areas, the extent of expected bending strength losses from the RBS can be estimated. One way to check the original strength design assumptions is to compare the nominal plastic moment of the full beam section, M_p^{nom} which is commonly used as an overall index of strength, to the actual beam end moment, M_c.

M_p^{nom} = maximum flexural strength (plastic moment) in beam based on nominal properties $F_y Z$ (of full section)

If a reasonable tolerance on the reduced beam section is maintained (say ± 5 percent of required z), M_c will approximately equal $C_f F_y^{act} S$ at the beam end by definition. The moment gradient provides this effect that interior reductions of beam capacity are partially recovered at the member end.

Past steel shape material surveys have shown that on the average, F_y^{act}/F_y = 55/50 = 1.1 for A572 Grade 50. (Ref. 8) Based on these observations, it can be generalized that the average actual yield will be 10 percent higher than nominal (minimum) F_y, i.e. $F_y^{act} = 1.1F_y$. Therefore, assuming Z/S = 1.1 and C_f = 1.0, results in the expected identity

$$M_c = F_y^{act} S = 1.1 F_y \frac{Z}{1.1} = F_y Z \qquad (12)$$

since the geometric shape factor difference is compensated for by the average expected material overstrength on yield.

More generally, the ratio between M_c/M_p^{nom} can be estimated from

$$C_f \left(\frac{F_y^{act}}{F_y}\right) \frac{S}{Z}$$

for a typical wide flange shape factor Z/S = 1.1 with Grade 50 steel:

C_f	$\left(\frac{F_y^{act}}{F_y}\right)$	$\frac{M_c}{M_p^{nom}}$
0.9	1.0	0.8
	1.1	0.9
1.0	1.0	0.9
	1.1	1.0

At worst, with C_f = 0.9 and no beam overstrength ($F_y^{act} = F_y$), no more than a 20 percent decrease in the nominal bending strengths relative to the original (unreduced) members is expected at the beam end (column face).

Thus, on average (with 10 percent overstrength), the actual beam end moment magnitude is not anticipated to be significantly below M_p^{nom} provided that excess flange removal beyond that required for connection ductility is avoided. The only presumption is that adequate control is imposed on the size and location of the RBS to permit the intended moment $M_c > C_f F_y^{act} S$ to develop at the beam end. Consequently, any initial frame analyses and code strength design checks assuming beam end M_p^{nom} should not be significantly affected, however, these should be independently assessed. Naturally, use of average yield strength ratios recognizes that specific beams will have higher or lower real values.

CONCLUSIONS

This paper outlines several basic strength principles that could be used in a convenient design of beams with reduced sections to achieve a proper balance between seismic ductility

and strength demand. First-order effects of moment continuity, beam span, and beam properties were included in a general systematic procedure. Other similar design formulations are possible. Due care must be exercised to avoid arbitrary or excessive flange reductions, to employ appropriate complete-joint-penetration groove welding and other load and design requirements at the beam-to-column connection in compliance with current building codes. Refs 9, 10, 11 and 12 give more recent and readily available sources for RBS test data and building applications. Appendix A extends the analysis to more fully include gravity load effects. Appendix B contains corollary guidelines for cover-plated details. Appendix C estimates the elastic stiffness loss for a beam. Appendix D presents another option of combining an RBS with beam end reinforcement. Ongoing and further research is expected to refine and/or extend these interim criteria to asymmetrical flange reductions, optimized cutout patterns, limitations, and other considerations.

The assistance of the Northridge Industry Research Fund, the Structural Shape Producers Council, the SAC Joint Venture, and the research community in the development of these concepts is acknowledged.

REFERENCES

1. Chen, S. J. & Yeh, C. H., *Enhancement of Ductility of Steel Beam-to-Column Connections for Seismic Resistance*, National Taiwan Institute of Technology, (presented at SSRC 1994 Annual Technical Session)
2. "Trade Arbed," *technical discussion/note*, June, 1994
3. U.S. Patent 5,148,642, Sept. 22, 1992
4. Plumier, A., *New Idea for Safe Structures in Seismic Zones*, University of Liege, IABSE Symposium, Brussels, Sept., 1990
5. Smith-Emery Co., *Reports on Four AISC Dogbone Tests*, Feb., 1996
6. Engelhardt, M. D. *Test Reports on Curved DogBone*, University of Texas-Austin, Dec.- Feb., 1996
7. American Institute of Steel Construction, *Northridge Steel Update I*, Oct., 1994
8. "Statistical Analysis of Tensile Data for Wide-Flange Structural Shapes", *University of Texas-Austin report for the Steel Shape Producers Council*, 1994
9. Federal Emergency Management Agency, "Interim Guidelines Advisory No. 1—Supplement to FEMA 267," *FEMA-267A*, January, 1997, SAC-96-03.
10. Iwankiw, Nestor R., and Carter, Charles J., "The Dogbone: A New Idea to Chew On", AISC *Modern Steel Construction*, April, 1996.
11. Engelhardt, M. D., Winneberger, T., Zekany, A. J. and Potyraj, T. J., "The Dogbone: Part II", AISC *Modern Steel Construction*, August, 1996.
12. Zekioglu, A., Mozaffarian, M., Le Chang, K., Uang, C. M., "Designing After Northridge," AISC *Modern Steel Construction*, March 1997.

Appendix A
Beam Gravity Load Considerations

The simple model developed in the body of this paper presupposes that lateral loading is the dominant factor. Full-scale connection test specimens are typically cantilevered beam-column assemblies that simulate a pure seismic loading. All other building structures are exposed to some combination of gravity and lateral load effects. This Appendix examines the consequences of gravity load effects in more detail, particularly on the shear coefficient c_v.

Consider again, a fixed-fixed beam, but now simultaneously subjected to both lateral and uniform gravity loads. An elastic superposition of their bending moments is shown.

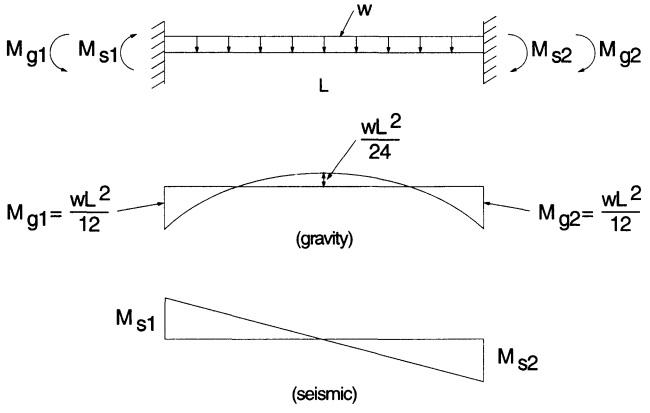

where

M_{g1}, M_{g2} = gravity load end moments = $wL^2/12$
M_{s1}, M_{s2} = seismic end moments
w = uniform gravity load

Because the gravity end moments are equal and opposite in direction (clockwise and counterclockwise), they are additive to the unidirectional lateral (seismic) moments on beam end 2 and are subtractive on the other end 1: (see AISC 1993 LRFD Specification, Commentary, pg. 6-234)

where

$M_{u1} = M_{s1} - M_{g1}$
$M_{u2} = M_{s2} + M_{g2}$
M_{u1}, M_{u2} = combined end moments

At this ultimate limit state, the combination of gravity and lateral (seismic) moments cannot exceed the beam plastic moment on the additive side:

$$M_{u2} = M_{s2} + M_{g2} = M_p^{act} \tag{A1}$$

Once the maximum beam bending strength is achieved gravity will affect internal plastic hinge details, such as the reduced section, and its moment transfer to the beam end in two ways: 1) increased beam shear V_p, and 2) additional loading imposed on the beam end segment. These will be examined separately, with $m_p = M_p^{act}$ at the reduced section and L' defined as the beam span between reduced sections, as before.

First, consider the total shear force at the internal plastic hinge that superimposes both seismic and gravity load components on the additive side.

$$V_s + V_g = V_p \tag{A2}$$

where

V_s, V_g = shear at RBS due to only seismic and gravity loads, respectively.

Equation 3 already defines $V_s = 2M_s / L'$. For a gravity-only uniform load on a fixed end beam, the elastic end moment at the RBS is

$$M_g = w\frac{(L^*)^2}{12}$$

$$(L^*)^2 = [(L' - e)^2 - 3e^2] = [L^2 - 6e(L - e)]$$

and

$$V_g = \frac{wL'}{2} = \frac{6M_gL'}{(L^*)^2} \tag{A3}$$

Substitution into Equation A2 results in

$$\frac{2M_s}{L'} + \frac{6M_gL'}{(L^*)^2} = V_p$$

which can then be expressed in terms of m_p and M_g using $M_s = (m_p - M_g)$ as

$$V_p = \frac{2m_p}{L'} + M_g\left(\frac{6L'}{(L^*)^2} - \frac{2}{L'}\right) \tag{A4}$$

To check for the seismic only case

$$(M_g = 0),\ V_p = \frac{2m_p}{L'},$$

and for gravity only,

$$(m_p = M_g),\ V_p = \frac{6m_pL'}{(L^*)^2},$$

Equation A4 can be used to determine this exact shear at the RBS for combinations of gravity and seismic loads.

A simpler and conservative shear calculation can also be made by just adding the uniform load reaction:

$$V_p = \frac{2m_p}{L'} + \frac{wL'}{2} \tag{A5}$$

Such an approximation ignores the fact that the gravity load moment is additive to the seismic moment only at one beam end, hence the $2m_p / L'$ term is larger than statics would require. This fact is also obvious by comparison with the exact (A4), wherein the $-2M_g / L'$ term corrects for this bending asymmetry. For stiffness controlled members wherein $M_g / m_p \leq 0.10$, this approximation provides reasonable shear forces that are usually within 10 percent (conservative) of the exact (A4).

In order to be consistent with this paper's RBS methodology, the V_p shear force, including uniform gravity effects, is converted into the c_v coefficient. This can easily be done by dividing (A4) & (A5) by m_p / L':

$$\text{exact } c_v = 2 + \frac{M_g}{m_p}\left(\frac{6L'^2}{(L^*)^2} - 2\right) \tag{A6}$$

$$\text{approx. } c_v = 2 + \frac{wL'^2}{2m_p} \tag{A7}$$

Gravity effects will always increase the RBS shear force, V_p, above the pure seismic level of $2m_p / L'$, and correspondingly $c_v > 2.0$. Any concentrated loads also need to be similarly analyzed.

For seismic frames controlled by stiffness with an L / d in the range of 10, the design gravity moment for office occupancy is typically expected not to exceed about 10 percent of the beam capacity, i.e. $M_g / m_p \leq 0.10$. Under such conditions, and with the RBS $e / d = 1.0$, c_v will be about 2.65, while the approximate value from (A7) will be 2.85, or about 8 percent higher. The RBS flange size, r, will be proportionally affected. For shorter beam spans with L / d between 5 and 10, this gravity shear effect will quickly escalate to c_v values as high as 7. These represent a range that might be encountered; actual design requirements will depend on the applicable building code and project specifications. Beam and connection shear strength need to be properly checked.

The second issue is the gravity effects on the bending moment between the internal plastic hinge at e and the beam end support.

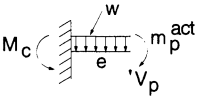

Include expected uniform gravity load w over segment end distance e, as shown. The M_c increase on the additive end (M_{u2}) amounts to $we^2 / 2$, and there would be a like decrease on the subtractive end (M_{u1}).

With maximum (e / d) set at unity and assuming an $L / d = 10$, $e = 0.1L$, the end moment increment for this secondary bending effect may then be approximated as

$$\Delta M_c = \frac{w(0.1L)^2}{2} = \frac{wL^2}{200} = 0.06\left(\frac{wL^2}{12}\right) = 0.06M_{g2}$$

or 6 percent of the elastic fixed-end moment for a uniformly loaded beam.

As discussed earlier, the end gravity moment is often less than $0.10M_p$ for a seismic frame beam governed by stiffness. Under these typical conditions, ΔM_c can be approximated as $0.06(0.1M_p)$, or $0.006M_p$, about a 0.5 percent deviation from the beam design moment.

Since this trivial increase occurs only near one beam end, it can be considered a secondary factor.

In conclusion, gravity load effects, though often minor relative to high seismicity demands, must be included in the RBS design, as in other details.

Appendix B
Corollary for Cover-Plated Connections (without RBS)

The fundamental detailing considerations developed previously for the RBS are also applicable, with some modifications, to the reinforced (cover-plated) moment connections already verified by the 1994 UTA research (Ref. 7), and its similar counterparts (vertical ribs & haunches). For example, consider the "rule-of-thumb" contained in Ref. 7 "to size the connection reinforcement so that the elastic section modulus of the total reinforced cross-section is approximately 1.5 to 2.0 times the elastic section modulus of the unreinforced beam."

All the test specimen beams from Ref. 7 were W36×150 (d = 35.85 in.), with a cantilever arm of 134 in. (L = 2 × 134 = 268 in.), translating to an equivalent L/d of about 7.5. The internal hinge location was at approximately d away from the beam end ($d/2$ clear distance plus $d/2$ hinge length), thus e/d = 1. Recall Equations 5 and 6 that relate the beam end moment to the internal plastic hinge, which for the cover-plated beam end without an RBS becomes:

$$\alpha\beta F_y^{\ act} Z = M_c = C_f F_y^{\ act} \overline{S} \qquad \text{(B1)}$$

The only change from Equation (6) is replacing z with Z, since the full beam plastic moment is developed at the internal hinge, and replacing S with $\overline{S}$, the reinforced section modulus at the beam end. With end reinforcement, there is no need to provide a lower design limit on C_f (as done previously with 0.9 for RBS.) The bending moment demand at the column face, M_c, is still driven by the internal plastic hinge, $\alpha\beta F_y^{\ act} Z$. Dividing Equation (B1) by S and rearranging results in

$$\frac{\overline{S}}{S} = \frac{\alpha\beta\left(\frac{Z}{S}\right)}{C_f} \qquad \text{(B2)}$$

which is simply the reciprocal of (z/Z) per Equation 6. It results in the following reinforcement ratios to form an internal plastic hinge for some typical L/d values with e/d = 1, β = 1.1, C_f = 1, c_v = 2, and Z/S = 1.15 for a W36×150 beam. Again, the beam strength $F_y^{\ act}$ cancels and does not affect this calculation.

L/d	$\overline{S}/S$
20	1.41
15	1.46
10	1.58
7.5	1.73

Note that the 1994 Texas specimens by this simple calculation require about 73 percent elastic section modulus reinforcement for the more severe L/d = 7.5, well within the published 1.5–2.0 "rule-of-thumb" range. However, the advantage of this computation is that the actual (higher) beam L/d ratios may offer some relief to minimize cover-plating sizes.

Again, parallel to the reduced section, a general relationship can be developed between the total ($\overline{S}/S$), or approximately ($\overline{I}/I$), and a percent increase in the flange area and moment of inertia with cover-plates. Using moment of inertias by parts, this can be stated as:

$$\frac{\overline{I}_f}{I} + \frac{I_w}{I} = \frac{\overline{I}}{I} \qquad \text{(B3)}$$

where

$\overline{I}_f$ = moment of inertia of original beam flange and reinforcement, in.^{4}
I_w = moment of inertia of beam web, in.^{4}
I = total moment of inertia of original beam, in.^{4}
$\overline{I}$ = total moment of inertia of reinforced beam, in.^{4}

Let $\overline{I}_f = sI_f$

where

I_f = moment of inertia of original beam due to flanges, in.^{4}
s = percent increase in flange area due to cover plates (when based only on flange thickness, assuming approximately same cover plate width, $s = (t_f + t_p)/t_f > 1.0$
t_p = flange cover plate thickness = $t_f(s-1)$, in.
t_f = beam flange thickness, in.

then the following results

$$s\left(\frac{I_f}{I}\right) + \frac{I_w}{I} = \frac{\overline{I}}{I} \qquad \text{(B4)}$$

		s	$\left(\frac{I_f}{I}\right)$	$\left(\frac{I_w}{I}\right)$	$\left(\frac{\bar{I}}{I}\right)$
A	20%	1.2	0.8	0.2	1.16
	flange thickness	1.2	0.7	0.3	1.14
	increase	1.2	0.6	0.4	1.12
B	40%	1.4	0.8	0.2	1.32
	flange thickness	1.4	0.7	0.3	1.28
	increase	1.4	0.6	0.4	1.24
C	60%	1.6	0.8	0.2	1.48
	flange thickness	1.6	0.7	0.3	1.42
	increase	1.6	0.6	0.4	1.36
D	80%	1.8	0.8	0.2	1.64
	flange thickness	1.8	0.7	0.3	1.56
	increase	1.8	0.6	0.4	1.48
E	100%	2.0	0.8	0.2	1.8
	flange thickness	2.0	0.7	0.3	1.7
	increase	2.0	0.6	0.4	1.6

Notice again that the magnitude of the flange strengthening is somewhat diluted in the overall increase of section flexural inertia ($\bar{I}/I$) and ($\bar{S}/S$). This convenient table demonstrates that matching the cover plate thickness to the beam flange thickness ($s = 2$) with similar flange widths provides an amply conservative detail for even an L/d as low as 7.5. Such calculations may justify cover plate thicknesses less than matching those of the beam flange.

Despite possible end stress reductions, overdesign of the cover-plates (excessive thickness) may be undesirable since it will result in additional welding and connection restraint that may be counterproductive. A reinforced detail also automatically causes higher beam end moments than M_p that need to be equilibrated throughout the framing system.

Appendix D discusses use of lighter end reinforcement in conjunction with an RBS.

Appendix C
Elastic Stiffness Change for Reduced Beam Section

Possible member and frame stiffness losses may initially be a concern to some with this new detail. The following simple analysis can help to analytically demonstrate that such a change in the elastic stiffness of an RBS member is marginal for the practical purposes of drift evaluation.

Consider again a fixed-end beam subject to a unit end rotation. The classical conjugate beam method can be used to conveniently derive the usual rotational stiffness coefficients for an elastic prismatic member (uniform moment of inertia, I) of $4EI/L$ and $2EI/L$. Recall that the (M/EI) diagram serves as the loading for the conjugate beam with superposition of the two end stiffness coefficients K_{11} and K_{21}.

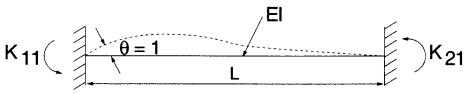

real beam

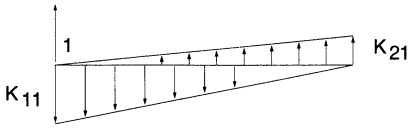

conjugate beam

$$\Sigma M_1 = 0: \left(\frac{K_{21}}{EI}\right)\left(\frac{L}{2}\right)\left(\frac{2L}{3}\right) = \frac{K_{11}}{EI}\left(\frac{L}{2}\right)\left(\frac{L}{3}\right)$$

$$\frac{K_{21}}{3} = \frac{K_{11}}{6}$$

$$K_{21} = \frac{K_{11}}{2}$$

$$\Sigma F = 0: 1 + \left(\frac{K_{21}}{EI}\right)\left(\frac{L}{2}\right) = \frac{K_{11}}{EI}\left(\frac{L}{2}\right)$$

$$1 + \left(\frac{K_{11}}{2EI}\right)\frac{L}{2} = \frac{K_{11}}{EI}\left(\frac{L}{2}\right)$$

$$1 = \frac{K_{11}L}{4EI}$$

$$\frac{4EI}{L} = K_{11}$$

$$\& \; K_{21} = \frac{2EI}{L}$$

Now, assume idealized reduced beam with uniform (z/Z) = 0.75 (about 35 percent flange reduction) over a distance of $0.75d$, at $c = d$ away from beam end, for L/d = $10(d = 0.1L)$. The reduction in plastic section modulus converts to a similar reduction in moment of inertia. Repeating the previous conjugate beam analysis for this nonprismatic member results in approximately a 7 percent reduction of rotational end stiffness (average depth rectangles conveniently approximate the extra (M/EI) "load" at the reduced sections).

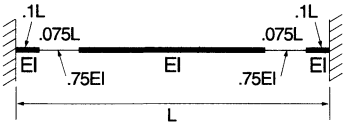

real beam

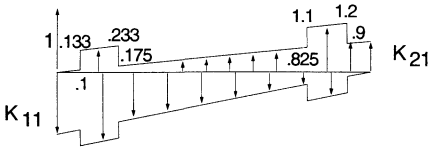

conjugate beam

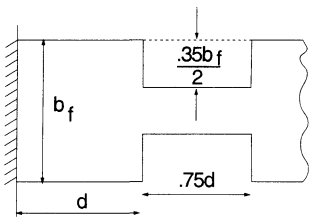

The reduced beam contours suggested in Fig. 1 always provide for transition regions at both ends of the RBS, not the abrupt step drop over a distance of $0.75d$, crudely assumed here, and c will be less than d (down to 0.25). Hence, more accurately computed stiffness reductions for specific conditions would be less, probably on the order of 5 percent or lower. Ref. 1 indicates that this member stiffness loss is only on the order of 3 percent for the specimens under study. Such marginal deviations are well within normal expectations of analysis/computational tolerances, and might, therefore, reasonably be neglected. Conversely, one might claim that the usual discounting of available positive stiffness contributions from nonstructural items, as well as the gravity (floor) system, more than compensates for this localized effect. Otherwise, a more refined structural model with non-prismatic beam properties can be used to check the frame drift.

Future frame analyses should more rigorously study the dynamic nonlinear effects of RBS under earthquake time-history input. Comparisons of period shift, lateral displacements (drift), base shear, inelasticity and ultimate load between the usual rigid frame and its RBS counterpart would be informative in further quantifying the hypothesis that the strength and stiffness changes introduced by an RBS frame are minor and negligible.

Appendix D
Combination Detail (RBS With Nominal End Reinforcement)

Two possibilities may necessitate additional end detailing modification to supplement the RBS. One is to further limit the stress in the beam to column welded connection to a value substantially below nominal yield of the beam (F_y). The second reason is the nature of the frame design itself (i.e. short spans, larger depth, low L/d) that could result in an excessive RBS (greater than 50 percent) to maintain moment continuity. Either one or both of these situations could be addressed through an RBS in combination with light reinforcement (ribs, haunches, or cover plates) of the beam end. Such a combination detail also provides for a degree of redundancy in the ductility mechanism and for more modest reinforcing and RBS requirements.

For a combination detail, the end bending moment, M_c, is still governed by basic moment continuity derived from the selected RBS at the internal plastic hinge. However, the nominal stress at the column face is controlled (reduced) through the type and amount of provided end reinforcement. The calculated elastic bending stress at the column face is

$$f_c = \frac{M_c}{\bar{S}} = \frac{\alpha\beta F_y^{\,act} z}{\bar{S}} \qquad \text{(D1)}$$

where

$f_c^{\,max}$ = maximum elastic stress at column face, ksi
$\bar{S}$ = elastic section modulus of reinforced beam end (as in Appendix B), in.[3]
$M_c = \alpha\beta F_y^{\,act} z$ (from Equation 5b), beam end moment at column face, kip-in.

With a combination detail, one first selects a convenient, or reasonable, RBS size and location, and subsequently, transfers these assumed load demands to the beam end moment M_c. From this strength demand, an elastic stress calculation for f_c determines the required end reinforcement ratio ($\bar{S}/S$) as

$$f_c^{\,max} = \frac{\alpha\beta F_y^{\,act}\left(\frac{z}{Z}\right)^* Z}{S} = \frac{\alpha\beta F_y^{\,act}\left(\frac{z}{Z}\right)^*\left(\frac{Z}{S}\right) S}{S}$$

$(z/Z)^*$ = selected RBS reduction, = 1 if RBS not used
Z/S = beam shape factor

or

$$\left(\frac{\bar{S}}{S}\right) = \frac{\alpha\beta F_y^{\,act}\left(\frac{z}{Z}\right)^*\left(\frac{Z}{S}\right)}{f_c^{\,max}} \qquad \text{(D2)}$$

For example, if $F_y^{\,act} = 1.1F_y = 55$ ksi for nominal $F_y = 50$ ksi, $\alpha = 1.2$, $\beta = 1.1$, $(z/S) = 0.8$ (30 percent flange reduction), and $f_c^{\,max} = 40$ ksi, Equation (D2) results in a required reinforcement ratio ($\bar{S}/S$) of 1.6. The above equation is similar to Equation (B2), the only difference being that Equation (D2) includes the $(z/Z)^*$ factor for the RBS and replaces C_f by the equivalent ($f_c^{\,max}/F_y^{\,act}$). Such design tradeoffs among calculated end connection stress, type and amount of reinforcement, size and location of RBS can be more completely explored through consideration of this more general formulation for a combination detail.